

DECOHERENCE AND ENERGY LOSS IN QCD CASCADES IN NUCLEAR COLLISIONS

A. Leonidov^(a,b), V. Nechitailo^(a,b)

(a) *Theoretical Physics Department, P.N. Lebedev Physics Institute,
Moscow, Russia*

(b) *Institute of Theoretical and Experimental Physics, Moscow, Russia*

Abstract

The medium modifications in the properties of QCD cascades are considered. In particular, the changes in the intrajet rapidity distributions due to medium-induced decoherence, collisional losses of cascade gluons and those of final prehadrons are analyzed.

1 Introduction

One of the most exciting experimental discoveries at RHIC are the dramatic changes in the patterns of energy flow in the events with large transverse energy. The simplest and most discussed related effect is the so-called jet quenching, the attenuation of hadrons with moderated and large transverse momenta, see the recent experimental review [1] and the theoretical reviews [2, 4, 3, 5, 6, 7] devoted to this problem. Generically the events with large transverse energies are jetty, i.e. are characterized by collimated bunches of hadrons. A description of intrajet properties of high energy jets in usual QCD vacuum [8] belongs to the most successful applications of perturbative QCD. The detailed picture of parton cascade dynamics including fine details such as a destructive quantum interference leading to an angular ordering in sequential gluon decays was worked out and shown to successfully explain experimental data on intrajet spectra and multiplicity distributions. This explains a great interest in studying the modifications of intrajet properties of QCD jets produced in high energy nuclear collisions in which QCD cascades develop in high density environment. Experimental studies of this problem have been performed at RHIC [9] and are planned at LHC [10].

On the theoretical side, in order to study the medium-induced modifications, one needs to work out the corresponding generalization of the formalism of the in-vacuum QCD. The presence of dense medium could influence the evolution of a cascade in two ways. First, the presence of the medium facilitates cascading by creating additional phase space for gluon emission. Second, there could be a non-radiative energy loss (gain) due to elastic interactions of the projectile with the modes of the medium. To account for interactions of the perturbative degrees of freedom in the evolving jet with the nonperturbative soft modes and/or medium one has to introduce an explicit mechanism of interaction between the partonic cascade and the environment.

The most detailed studies of in-vacuum QCD cascades are performed with the help of the Monte-Carlo simulations. The two most popular versions of these MC generators are PYTHIA [11] and HERWIG [12]. Both of them implement a key property of in-vacuum QCD jets, the angular ordering, that in the modern versions is directly built in, see a detailed discussion in [16] and in the Appendix of the present paper. The first PYTHIA-based MC program including the effects of medium-induced radiative energy loss was PYQUEN [13]. Recently there appeared several MC generators treating the medium-induced effects in the QCD cascades, in particular the PYTHIA-based JEWEL [14] and Q-PYTHIA [15] and the HERWIG-based "Q-HERWIG" [16]. In the present paper we have used the object-oriented code realizing the 'global' 'constrained' mass-ordered version of PYTHIA im-

plemented in JEWEL [14]. All of the above-listed MC generators take into account the medium-induced radiative energy loss that is believed to be a major source of the energy loss; JEWEL, in addition, includes the effects of rescattering of cascade particles on those in the medium. The generic effect due to the medium-related interactions is the softening of intrajet particle spectra accompanied by the transverse broadening of jets.

Let us note that for the case of non-radiative energy loss a corresponding modification of Altarelli-Parisi equations, constructed in analogy with a theory of ionization losses in electromagnetic cascades [17], was considered in [18, 19] where spectra and multiplicity distributions of QCD jets in a dissipative medium were studied.

The focus of the present paper is on the analysis of some medium-induced modifications in the evolution of QCD cascades related to the fine structure of the spatiotemporal pattern of the in-medium QCD cascade, in particular on the substantial softening of the intrajet rapidity distribution.

In the paragraph 2.1 we describe the basic features of the model of in-medium QCD cascade used in our simulations.

In the paragraph 2.2 we give the detailed description of the simulation of the mass-ordered QCD cascade.

In the paragraph 2.3 we discuss the substantial softening of the intrajet rapidity distributions due to decoherence effects leading to the disappearance of the angular ordering.

In the paragraph 2.4 we consider the effects of the collisional energy loss as related to the spatiotemporal pattern of the in-medium QCD cascade.

We conclude the paper with the short summary of the results obtained and of the problems to be addressed in the near future.

2 Decoherence and energy loss in in-medium QCD cascade

In the present paper we will concentrate on discussing the properties of the timelike in-medium QCD cascades. The physical origin of the cascading process is the intense gluon radiation of a high energy parton created in a hard subprocess. Operationally one can think of this radiation cascade as of equipping the initial parton with energy E_0 with some invariant mass Q_0^2 that is shaken off through decays into partons with lower invariant masses until reaching some non-perturbative scale $Q_h/2$ at which preconfined colorless clusters are formed.

When considering the properties of the in-medium QCD cascades one has

to deal with several mechanisms modifying the in-vacuum intrajet characteristics. These are, in particular, the loss of quantum coherence and the resulting loss of angular ordering, collisional and radiative energy losses. In the present paper we shall focus on studying the impact of decoherence and collisional energy loss of partons and final prehadrons. The main motivation is to analyze the dependence of observable quantities such as intrajet particle distributions, jet energy and multiplicity on the spatiotemporal pattern of the cascade, in particular on the distance from the origin of the cascade to the border of the hot dense fireball or, equivalently, the time interval during which the development of the cascade takes place inside the medium. To get a feeling for the corresponding physics, let us consider, for example, a gluon with the energy $E_0 = 100$ GeV equipped with a typical initial invariant mass $Q_0 = 10$ GeV. This gluon will on the average decay at $\tau_0 \sim E_0/Q_0^2 = 1 \text{ GeV}^{-1} \simeq 0.2$ fm, so that if the vertex in which the initial hard gluon was generated was sufficiently far (several fermies) from the surface of hot fireball, a significant part of cascade vertices will be generated inside the medium.

2.1 The model

The key elements of the model developed in the paper are illustrated in Fig. 1.

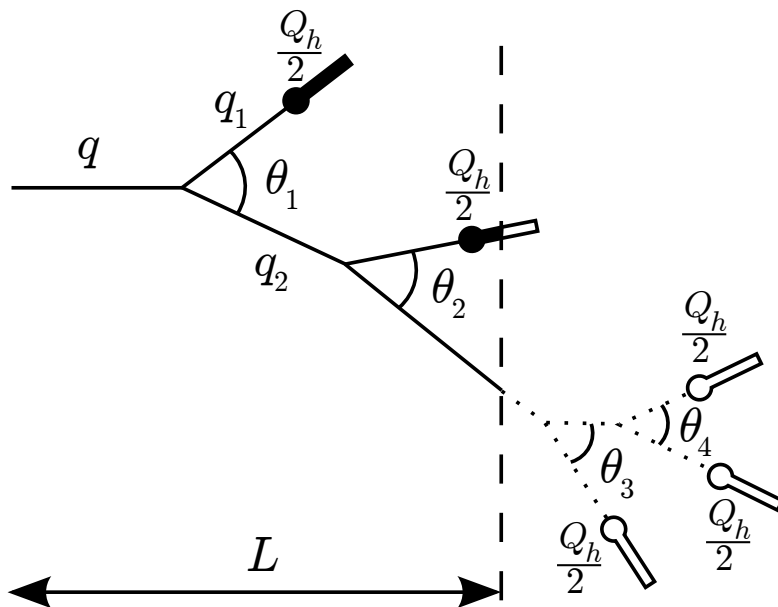


Figure 1: A sketch of the in-medium QCD cascade.

The area to the left of the vertical dashed line is the region filled with

dense parton matter where modifications of cascade properties take place. To the right of this line is the region of usual vacuum in which one has usual unmodified QCD cascade. The cascade is assumed to be initiated at the distance L from the medium-vacuum interface surface.

The considered modifications of cascade properties inside the medium are related to several mechanisms: decoherence due to color randomization, collisional losses of cascading gluons and those of final prehadrons.

2.1.1 Space-time pattern.

To determine whether a given line is still inside the medium or has already left it, one needs to set up a clock counting time along the cascade. The only possibility of associating a spatiotemporal pattern with the cascade is to use the lifetime τ of a virtual parton which, for a parton with the energy E and virtuality Q^2 that has been created in the decay of its parent parton with the virtuality Q_{par}^2 , reads

$$\tau = E \left(\frac{1}{Q^2} - \frac{1}{Q_{\text{par}}^2} \right) \quad (1)$$

The lifetime of the initial parton is taken to be $\tau_{\text{in}} = E_{\text{in}}/Q_{\text{in}}^2$. For example, the time τ_h at which the parton with the momentum q_1 in Fig. 1 produced the final prehadron is

$$\tau_h = E_0 \frac{1}{Q_0^2} + E_1 \left(\frac{4}{Q_h^2} - \frac{1}{Q_0^2} \right) = \frac{E_0}{Q_0^2} \left[1 + z \left(\frac{4Q_0^2}{Q_h^2} - 1 \right) \right]$$

where $z \equiv E_1/E_0$. For the parton under discussion it happened that $\tau_h < L$ so that both its formation at time E_0/Q_0^2 and its decay into final prehadron took place inside the medium.

2.1.2 Decoherence due to color randomization

For decays taking place inside the medium such as those of gluons with the momenta q and q_1 the angular ordering is absent. This means that, e.g., the magnitude of the angle θ_2 is not restricted by that of the angle θ_1 . The corresponding effects will be discussed in the paragraph 2.3.

2.1.3 Collisional losses of cascading gluons

The gluons propagating in the medium (solid lines) experience, before converting to final prehadrons (black circles) collisional energy loss. The corresponding effects will be considered in the paragraph 2.4.

2.1.4 Collisional losses of final prehadrons

The final prehadrons formed inside the medium, such as, e.g., that formed by the gluon initially having the momentum q_1 , experience the medium-induced collisional loss and, if having insufficient energy, do not leave the medium. The effects related to the prehadron collisional energy loss are discussed in the paragraph 2.4.

2.2 Mass-ordered QCD cascade

In this paragraph we describe the procedure of generating a mass-ordered gluon cascade we employ.

The cascade evolution goes through a sequence of decays $q \Rightarrow q_1 + q_2$, where $q = (E, \vec{q})$ is a four-momentum of the parent gluon and $q_{1(2)}$ are those of the daughter ones. We study the timelike evolution in which cascading reshuffles the initial jet virtuality in such a way that at each decay one has $q^2 > q_1^2 + q_2^2$, see below. The cascading process at a given branch stops when a virtuality of the last parton reaches a threshold level Q_h^2 , i.e. no decay into two partons with minimal virtuality $Q_h^2/4$ can occur¹. The key property of the in-vacuum QCD cascades, effective angular ordering of subsequent decays due to color coherence, is not automatically taken into account in the mass-ordered evolution and has to be enforced explicitly by accepting only those generated decays for which the condition of angular ordering does hold.

As the angular ordering is checked only a posteriori, the restrictions imposed on initially generated decays are purely kinematical so that for the decay $q \rightarrow q_1 + q_2$ the splitting variable $z = E_1/E \equiv 1 - E_2/E$ should lie in the interval

$$\tilde{z}_-(E, Q^2 | Q_1^2, Q_2^2) < z < \tilde{z}_+(E, Q^2 | Q_1^2, Q_2^2) \quad (2)$$

where

$$\tilde{z}_\pm(E, Q^2 | Q_1^2, Q_2^2) = \frac{1}{2} \left(1 + \frac{q_+ q_-}{Q^2} \pm \sqrt{\left(1 - \frac{Q^2}{E^2}\right) \left(1 - \frac{q_+^2}{Q^2}\right) \left(1 - \frac{q_-^2}{Q^2}\right)} \right), \quad (3)$$

$q_\pm = \sqrt{Q_1^2} \pm \sqrt{Q_2^2}$. The restriction (2) follows from the requirement of positivity of the square of transverse momentum generated in the decay. Let us also note that, as is immediately evident from (3), one has $Q_1 + Q_2 \leq Q$.

From equations (2,3) it follows that the full specification of a decay requires, generally speaking, knowledge of invariant masses of the offspring partons. In our simulations we employ the so-called 'global' 'constrained'

¹By default the virtuality of such a last parton is set to $Q_h^2/4$.

prescription that uses both the exact restriction (2,3) and its simplified version in which $Q_{1,2}^2$ are replaced by the minimal invariant mass $Q_h^2/4$:

$$z_-(E, Q^2 | Q_h^2) < z < z_+(E, Q^2 | Q_h^2) \quad (4)$$

where

$$z_{\pm}(E, Q^2 | Q_h^2) \equiv \tilde{z}_{\pm} \left(E, Q^2 \mid \frac{Q_h^2}{4}, \frac{Q_h^2}{4} \right) = \frac{1}{2} \left(1 \pm \sqrt{\left(1 - \frac{Q^2}{E^2}\right) \left(1 - \frac{Q_h^2}{Q^2}\right)} \right) \quad (5)$$

In particular, the simplified restrictions (4,5) are used when calculating the Sudakov formfactor

$$S(Q^2 | E, Q_{\max}^2; Q_h^2) = \exp \left[- \int_{Q^2}^{Q_{\max}^2} \frac{dt^2}{t^2} \int_{z_-(E, t^2 | Q_h^2)}^{z_+(E, t^2 | Q_h^2)} dz \frac{\alpha_s [z(1-z)t^2]}{2\pi} N_c K(z) \right]. \quad (6)$$

The equation (6) defines the probability to split into two gluons with virtualities $Q_h/2$ for a gluon with the energy E having a virtuality Q^2 restricted by condition $Q_h^2 < Q^2 < Q_{\max}^2$. In (6) $N_c = 3$ is the number of colors and $K(z) = \frac{1}{z(1-z)} - 2 + z(1-z)$ is the gluon splitting function.

The explicit procedure we employ to generate an in-vacuum mass-ordered gluon cascade is as follows:

1. First one draws, using (4,5,6), the scale Q^2 at which the gluon under consideration branches into two new gluons. Let us note that at this step one fixes the lifetime of the gluon $\tau = E(1/Q^2 - 1/Q_{\text{par}}^2)$.
2. One draws the value of the splitting variable z determining the energies of the offspring gluons $E_1 = zE$ and $z_2 = (1-z)E$.
3. With the energies of the offspring gluons fixed, one draws their final invariant masses $Q_{1,2}^2$ and, therefore, fix their lifetimes

$$\tau_{1,2} = E_{(1,2)} \left(\frac{1}{Q_{(1,2)}^2} - \frac{1}{Q^2} \right)$$

The values of $Q_{1,2}^2$ are accepted if they do not violate (3). In other case the maximum of $Q_{1,2}$ is redrawn until the condition (3) is satisfied².

²Let us note that such a procedure tends to exclude particles that simultaneously have big energies and virtualities. Indeed, let us assume that we have drawn some $Q \approx E$. This immediately leads to $z \approx 1/2$ and, therefore, makes it impossible to get $E_1 \approx E$ with $Q_1 \approx E_1$. At the same time if we drew $Q_1 = Q - Q_h/2$ and $Q_2 = Q_h/2$, we would get the case from (5): $z \approx 1 - Q_h/E$.

4. Finally, one ensures angular ordering by drawing the splitting variables for the decays of the offspring gluons $z_{1,2}$ and accepting them if they satisfy the inequalities

$$z_1(1 - z_1) > \frac{1 - z}{z} \left(\frac{Q_1^2}{Q^2} \right)$$

$$z_2(1 - z_2) > \frac{z}{1 - z} \left(\frac{Q_2^2}{Q^2} \right)$$

correspondingly.

2.3 Decoherence of in-medium QCD cascades

We have already mentioned that quantum coherence and resulting angular ordering of gluon emissions plays a crucial role in the physics of QCD jets. The violent environment created in ultrarelativistic heavy ion collisions acts as a source of random energy-momentum and color with respect to in-vacuum processes. This kind of random impact tends to ruin the phase tuning lying at the heart of quantum interference phenomena. The situations in which random external influences destroy the interference-related effects are very common in solid state physics. A well-studied example is provided by studying the physics of weak localization in the presence of random external impacts, see e.g. [22, 23]. Thus it is intuitively quite clear that the quantum coherence effects should be broken in the violent environment created in heavy ion collisions. This was first explicitly mentioned in [14], in which the origin of decoherence and ensuing disappearance of angular ordering was related to rescattering of cascading particles on scattering centers in the medium.

It is well known that in plasma physics the mean-field effects are typically much stronger than those related to scattering. It therefore of interest to point out to another source of decoherence, the randomness of the color of mean field. A quantitative argument is provided by comparing the characteristic times of color and momentum diffusion in dense strongly interacting matter, t_c and t_p correspondingly, that were calculated for quark-gluon plasma in [21]:

$$t_p \approx [4\alpha_s^2 T \ln(1/\alpha_s)]^{-1}$$

$$t_c \approx [3\alpha_s T \ln(m_E/m_M)]^{-1}, \quad (7)$$

where m_E is an electric screening mass and m_M - a (non-perturbative) magnetic screening one. Obviously the pace of color randomization is much

faster than that of momentum evolution and, therefore, collisional energy loss, $t_c \ll t_p$. This situation is similar to decoherence related to rotation of spin by random external magnetic field [24]. Therefore, when describing a propagation of a test high energy colored particle through plasma, one can assume that at time scales of order of t_c all coherent effects related to precise color matching are destroyed. The origin of angular ordering in the in-vacuum QCD cascades is exactly in such kind of precise color matching, therefore at the timescales $\tau \gtrsim t_c$ the color coherence is broken. Of course, the estimates for the timescales in (7) refer to equilibrated QCD matter considered in the hard loop approximation and are thus not too realistic. In the context of the present paper it is only important that (7) points out to color randomization as the fastest source of decoherence in the hot dense fireball.

In what follows we shall use a simplest assumption that angular ordering is always broken for gluon decays in QCD cascades that take place inside the hot dense medium. In this paragraph we consider the situation in which such breaking of angular coherence is the only medium-related effect in the gluon cascade. It is known for a long time that in the absence of angular ordering the properties of QCD cascades are very different from those when angular ordering is imposed [25]. In particular, the jet multiplicities decrease, but the strongest effect is related to the changes in intrajet energy distribution which experiences dramatic softening [25]. As in our considerations the effects of breaking of color ordering are present only for decays taking place inside the medium, the cumulative effect on energy distribution of final prehadrons, the strength of the above-mentioned softening should depend on the relative proportion of vertices generated inside the medium or, in other terms, on the distance L from the cascade origin to the border of the fireball.

In Fig. 2 we plot the distributions of final prehadrons in the rapidity $y = \ln(E_0/E)$ for gluon jets with the initial energy $E_0 = 100$ GeV and $L = 0.5, 1$ and 5 fm.

From the distributions in Fig. 2 we see that the effect of color decoherence is indeed very strong. Already at $L = 0.5$ fm the distribution is significantly different from the vacuum one and at larger L practically saturates. Thus, even in the absence of energy loss in terms of energy-momentum, the intrajet properties are significantly affected by the medium through color decoherence.

The changes in distribution over the rapidity $\ln(E_{\text{jet}}/E)$ shown in Fig. 2 reflect important changes in the spatiotemporal pattern of the jet. Indeed, from the inside-outside nature of particle production in which soft particles are produced faster than hard ones, cf. Eq. (1) one can conclude that the substantial softening of the rapidity distribution shown in Fig. 2 reflects an increased yield of short formation times of prehadrons. Thus it is of interest

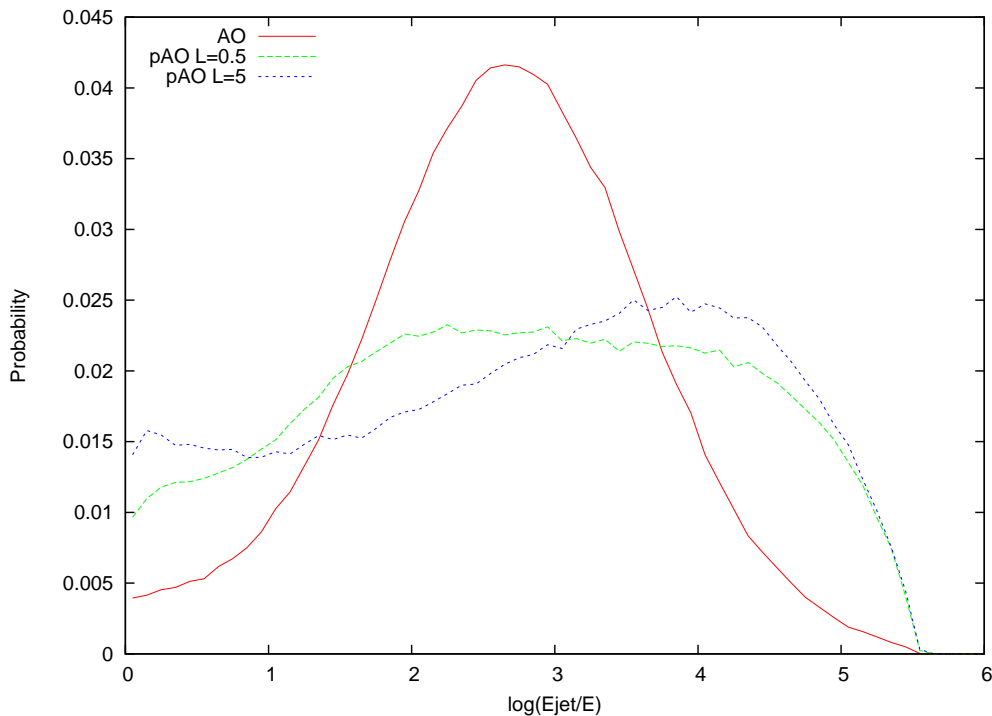


Figure 2: Rapidity distribution $P(y)$ of final prehadrons: 1) $L = 0$ fm, full angular ordering, red, solid; 2) $L = 0.5$ fm, partial angular ordering, green, dashed; 3) $L = 5$ fm, partial angular ordering, blue, dotted.

to consider the yield of prehadrons formed inside the medium of given length. This yield is plotted in Fig. 3 for jets with and without angular ordering.

2.4 Collisional losses in the in-medium QCD cascades

In this paragraph we shall make a crude estimate of the effects of the part of medium-induced energy loss which is proportional to the distance l that a parton or prehadron travel inside the medium. For simplicity, in analogy with QED cascades in matter, we shall term these losses as collisional losses. Radiative medium-induced losses are, at least at small times, proportional to l^2 and require a separate treatment. Usually one considers the radiative losses as dominant, so our restriction to the collisional ones provides an estimate of the minimal medium-induced energy loss.

In analogy with QED showers [26, 27], the partonic intrajet energy losses ΔE_p are described by the continuous distribution $\mathcal{P}(\Delta E_p, l | \mu_{\Delta E}, \sigma_{\Delta E})$. The parameters $(\mu_{\Delta E}, \sigma_{\Delta E})$ describe the mean energy loss and the corresponding standard deviation at the distance of 1 fm. In our simulations we use a simple

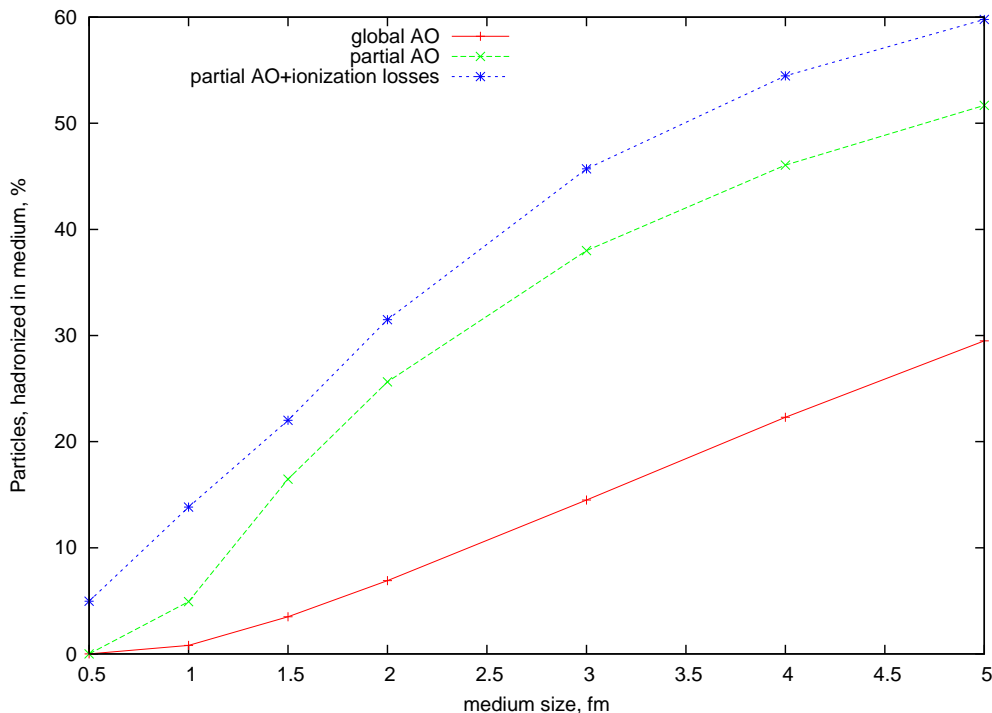


Figure 3: Relative yield of prehadrons formed inside the medium: 1) global angular ordering, red, solid; 2) partial angular ordering, green, dashed; 3) partial angular ordering and collisional losses, blue, dotted.

Gaussian parametrization of $\mathcal{P}(\Delta E, l | \mu_{\Delta E}, \sigma_{\Delta E})$:

$$\mathcal{P}(\Delta E_p, l | \mu_{\Delta E}, \sigma_{\Delta E}) = \nu \delta(\Delta E_p) + \frac{1}{\sqrt{2\pi}\sigma_{\Delta E}l} \exp\left\{-\frac{(\Delta E_p - \mu_{\Delta E}l)^2}{2\sigma_{\Delta E}^2l^2}\right\} \Theta(\Delta E_p) \quad (8)$$

where

$$\nu = \frac{1}{\sqrt{2\pi}} \int_1^\infty dx \exp(-x^2/2) = \frac{1}{2}(1 - \text{erf}(\sqrt{2}/2)) \approx 0.159$$

as we use only the case $\mu_{\Delta E} = \sigma_{\Delta E}$. The numerical values we chose in most of the simulations were $\mu_{\Delta E} = 1 \text{ GeV/fm}$ and $\sigma_{\Delta E}^2 = 1 \text{ GeV}^2/\text{fm}$.

The losses ΔE_h experienced by prehadrons formed inside the medium on their way out of the hot fireball were simply taken to be proportional to the distance they cover inside the medium, $\Delta E_h = 1 \text{ GeV/fm} \cdot l$.

Taking into account the softness of the majority of produced prehadrons that takes place even without taking into account the energy losses, just because of decoherence, an interesting question to address is how many prehadrons have enough energy to leave the medium when the energy losses

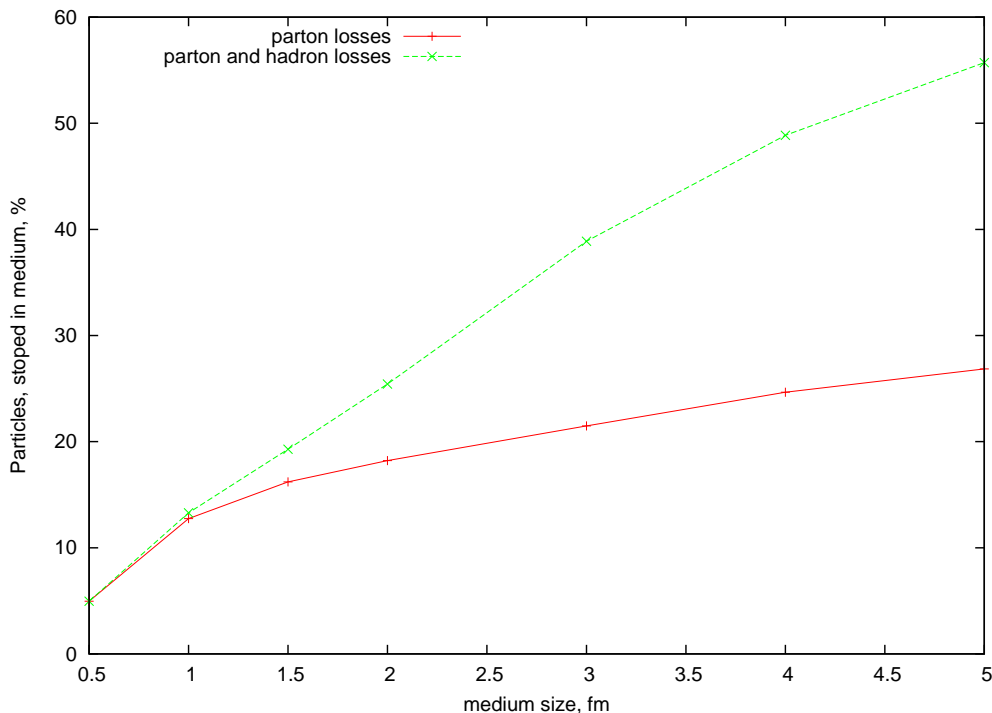


Figure 4: Relative yield of particles stopped inside the medium: 1) parton losses, red, solid; 2) parton and hadron losses, green, dashed.

are switched on. The simplest crude criterion of stopping one can use is $E_{\text{crit}} = Q_h/2$ so that the momentum of the corresponding parton or prehadron is zero. The corresponding yields are shown in Fig. 4.

We see that at large enough distances to the border of the fireball the effect is very significant: at $L = 5$ fm more than half of the final prehadrons are stopped inside the fireball. The effect of stopping is also clearly seen in Fig. 5 in which we plot the average multiplicity of final prehadrons inside the cone $\theta_{\text{jet}} = 0.7$.

For completeness in Fig. 6 we show the dependence of average energy within the cone of $\theta_{\text{jet}} = 0.7$ on L .

The additional softening incurred by energy losses does considerably change the shape of the rapidity distributions of final prehadrons. In Fig. 7 we plot the corresponding distributions at $L = 5$ fm and in Fig. 8 we illustrate the dependence of rapidity distribution taking into account all sources of energy loss on L .

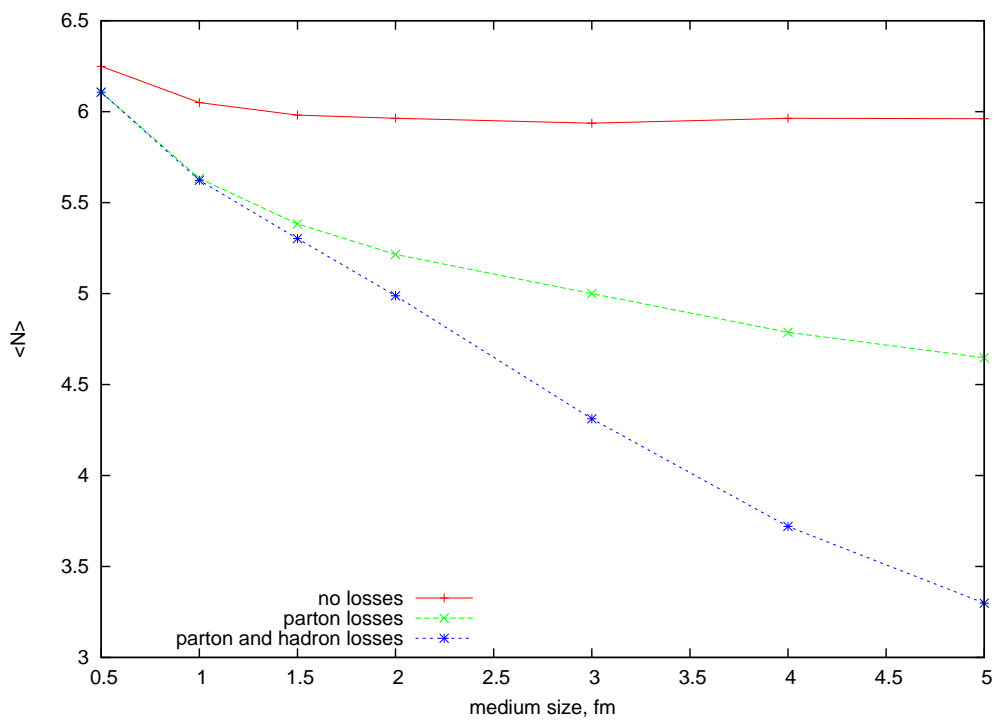


Figure 5: Mean jet multiplicity as a function of medium size: 1) no losses, red, solid; 2) intracascade parton losses, green, dashed; 3) intracascade and final state losses, blue, dotted.

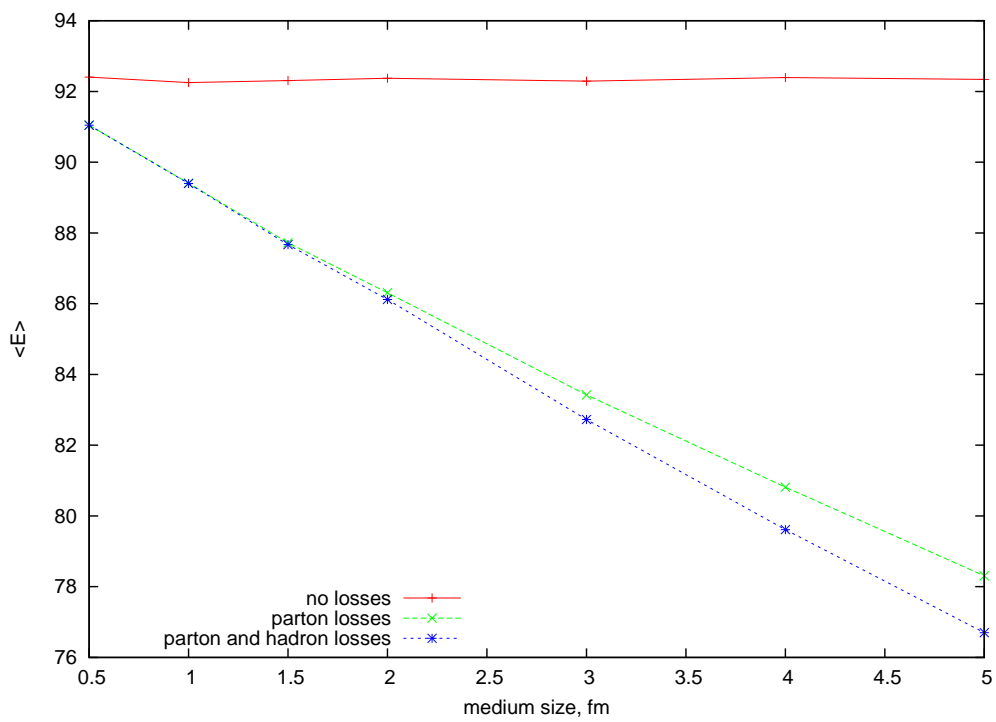


Figure 6: Mean jet energy as a function of medium size: 1) no losses, red, solid; 2) intracascade parton losses, green, dashed; intracascade and final state losses, blue, dotted.

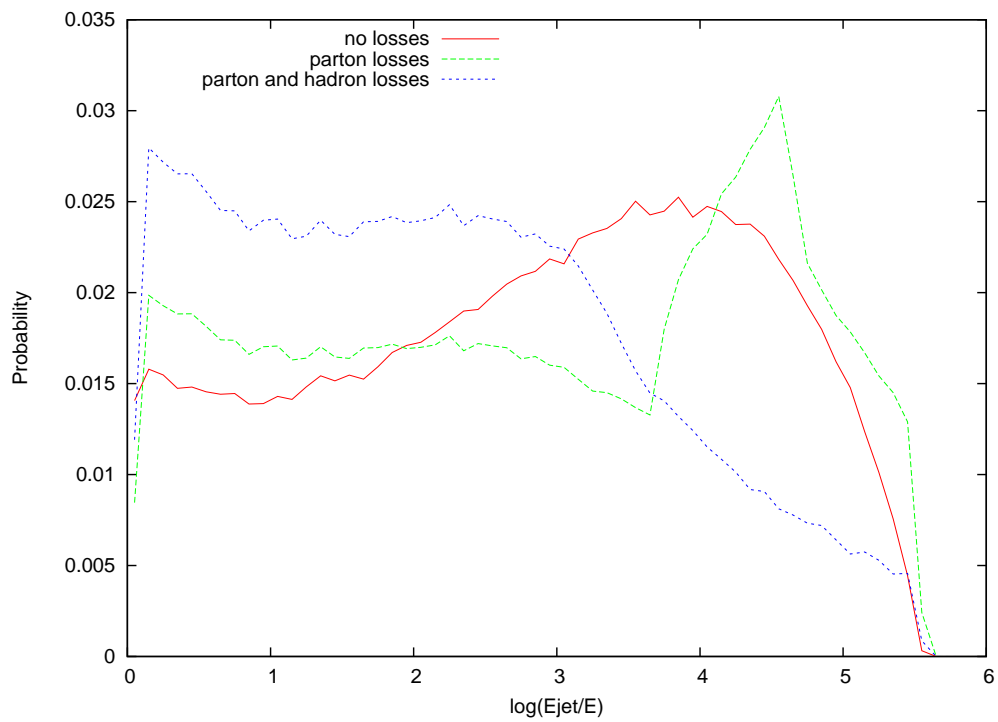


Figure 7: Rapidity distribution $P(y)$ of final prehadrons, cascade with partial angular ordering: 1) no losses, red, solid; 2) intracascade parton losses, green, dashed; 3) intracascade and final state losses, blue, dashed.

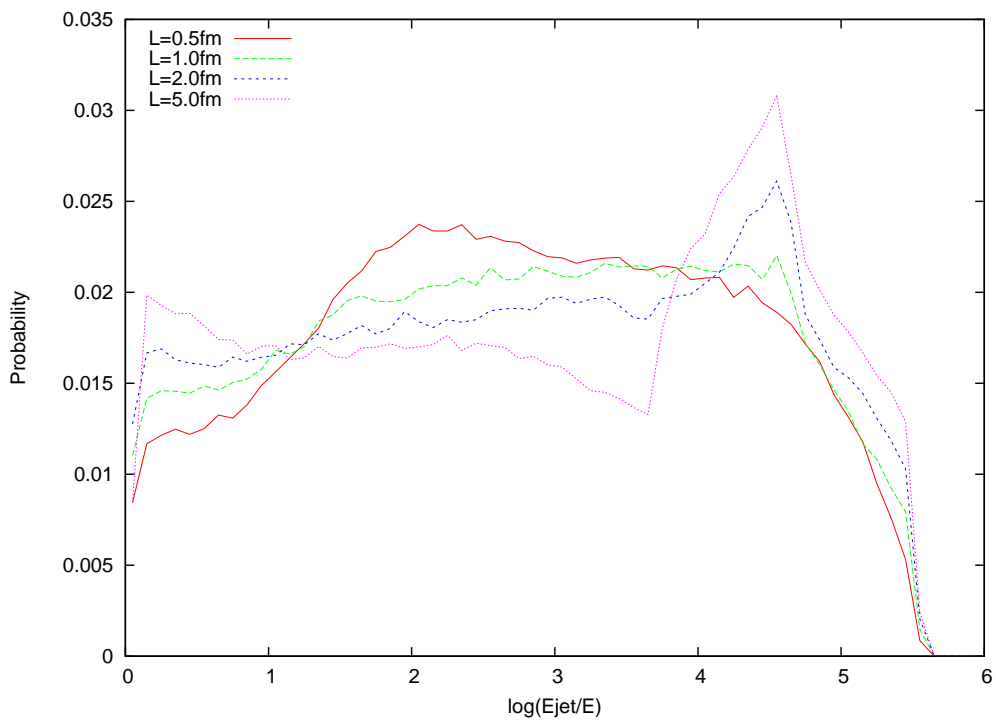


Figure 8: Rapidity distributions at different medium length L

3 Conclusions

The main goal of the present study was to analyze some medium-induced changes in the evolution of the in-medium QCD cascade.

In the focus of our attention was a detailed analysis of the medium-induced color decoherence and the ensuing disruption of angular ordering for the decays taking place inside the medium. We have shown that this effect leads to the substantial softening of the intrajet rapidity spectrum.

Another quantitatively important effect considered in the paper is that of the collisional losses of cascade gluons and of those final prehadrons that happened to be formed inside the medium. We have shown that, at variance with the widespread opinion that the dominant majority of the final hadrons form outside the hot and dense fireball, the yield of prehadrons formed inside the fireball is quite significant. Combined with the effect of partonic collisional loss, this leads to the substantial deformation of the rapidity spectra.

To make the analysis presented in this paper more complete one has, of course, take into account the medium-induced radiative losses. Work on this problem is currently in progress.

Acknowledgements

We are grateful to I.M. Dremin for very useful discussions.

The work was supported by the RFBR grants 06-02-17051, 08-02-91000, 09-02-00741 and the RAS program "Physics at the LHC collider".

Appendix

Let us discuss the approximations which made when "angular ordering" conditions is introduced. Recall that the "angular" variable³ which is used in Herwig and similar is written as

$$\xi \equiv \frac{(p_b, p_c)}{E_b E_c} = 1 - \frac{(\vec{p}_b, \vec{p}_c)}{E_b E_c} = 1 - \frac{1}{2} \frac{\vec{p}_a^2 - \vec{p}_b^2 - \vec{p}_c^2}{E_b E_c}, \quad (\text{A.1})$$

where we have used

$$\vec{p}_a^2 = (\vec{p}_b + \vec{p}_c)^2 = \vec{p}_b^2 + \vec{p}_c^2 + 2(\vec{p}_b, \vec{p}_c) \quad (\text{A.2})$$

The initial upper limit for ξ usually supposed as 1. This means that we consider the opening angles θ_a to be less then $\pi/2$ only. In this area the

³This is exactly the same variable for which the ordering was originally derived in [28]

conditions of angular ordering (θ) and $\sin \theta$ (or p_t or $\sin^2 \theta$) are equivalent. In terms of momenta we have for $\sin^2 \theta$

$$\sin^2 \theta_a = 1 - \frac{(\vec{p}_b, \vec{p}_c)^2}{\vec{p}_b^2 \vec{p}_c^2} = 1 - \frac{1}{4} \frac{(\vec{p}_a^2 - \vec{p}_b^2 - \vec{p}_c^2)^2}{\vec{p}_b^2 \vec{p}_c^2} \quad (\text{A.3})$$

where we again used (A.2).

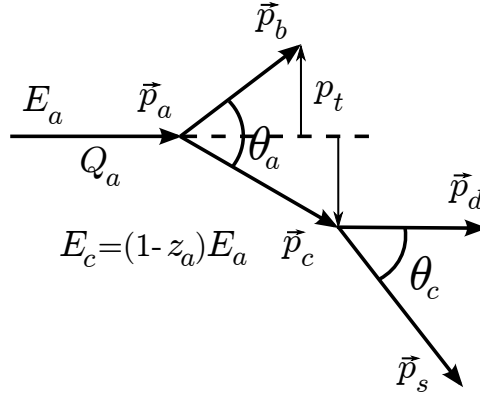


Figure 9: Angular ordering

As for considered angles $\vec{p}_a^2 - \vec{p}_b^2 - \vec{p}_c^2 > 0$ we can rewrite the ordering condition as following (see Figure for parton indexes)

$$\frac{\vec{p}_c^2 - \vec{p}_s^2 - \vec{p}_d^2}{|\vec{p}_s||\vec{p}_d|} \geq \frac{\vec{p}_a^2 - \vec{p}_b^2 - \vec{p}_c^2}{|\vec{p}_b||\vec{p}_c|} \quad (\text{A.4})$$

and for ξ variable

$$\frac{\vec{p}_c^2 - \vec{p}_s^2 - \vec{p}_d^2}{E_s E_d} \geq \frac{\vec{p}_a^2 - \vec{p}_b^2 - \vec{p}_c^2}{E_b E_c} \quad (\text{A.5})$$

Comparing (A.4) and (A.5) we see that ξ -ordering coincide with true angular ordering if we suppose $E \approx |\vec{p}|$ in denominators of (A.4). Which condition is stronger depends on the four ratios Q/E and can be different for different cases.

From other side

$$\vec{p}_a^2 - \vec{p}_b^2 - \vec{p}_c^2 = E_a^2 - E_b^2 - E_c^2 - Q_a^2 + Q_b^2 + Q_c^2 = 2E_b E_c - Q_a^2 + Q_b^2 + Q_c^2 \quad (\text{A.6})$$

where we have used energy conservation $E_a = E_b + E_c$. And we can rewrite condition (A.5) as following

$$\frac{Q_c^2 - Q_d^2 - Q_s^2}{E_s E_d} \leq \frac{Q_a^2 - Q_b^2 - Q_c^2}{E_b E_c} \quad (\text{A.7})$$

or taking into account that $E_s E_d = z_c(1-z_c)E_c^2$ and $E_b = z_a E_a = z_s \frac{E_c}{(1-z_a)}$,

$$\frac{Q_c^2 - Q_d^2 - Q_s^2}{z_c(1-z_c)} \leq \frac{(Q_a^2 - Q_b^2 - Q_c^2)(1-z_a)}{z_a} \quad (\text{A.8})$$

If we now suppose that $Q_a^2 \gg Q_b^2 + Q_c^2$ and $Q_s^2 \gg Q_d^2 + Q_a^2$ we get the conditions which is used in ‘‘Virtuality ordered’’ Pythia as angular ordering condition

$$\frac{Q_c^2}{z_c(1-z_c)} \leq \frac{Q_a^2(1-z_a)}{z_a} \quad (\text{A.9})$$

References

- [1] d’Enterria D arXiv:0902.2011 [nucl-ex]
- [2] R. Baier, D. Schiff, B.G. Zakharov, *Ann. Rev. Nucl. Part. Sci.* **50** (2000), 37
- [3] Kovner A, Wiedemann U A, ‘‘Gluon radiation and parton energy loss’’, in R.C. Hwa and X.-N. Wang (eds) ‘‘Quark Gluon Plasma 3’’, 192 (2003), arXiv:hep-ph/0304151
- [4] M. Gyulassy, I. Vitev, X.-N. Wang, B-W. Zhang, ‘‘Jet quenching and radiative energy loss in dense nuclear matter’’, in R.C. Hwa and X.-N. Wang (eds) ‘‘Quark Gluon Plasma 3’’, 123 (2003), arXiv:nucl-th/0302077
- [5] Casalderrey-Solana J, Salgado C A, arXiv:0712.3443 [hep-ph]
- [6] Wiedemann U A arXiv:0908.2306 [hep-ph]
- [7] Majumder A arXiv:1002.2206 [hep-ph]
- [8] Yu.L. Dokshitzer, V.A. Khoze, A.H. Mueller and S.I. Troyan, *Basics of perturbative QCD*, Edition Frontiers, 1991
- [9] J. Putschke, *Eur. Phys. J.* **C61** (2009), 629
E. Bruna, *Jet fragmentation in STAR going from p+p to Au=Au*, arXiv:0905.4763[nucl-ex]
E. Bruna, *Measurements of jet structure and fragmentation from full jet reconstruction in heavy ion collisions at RHIC*, arXiv:0907.4788[nucl-ex]
- [10] M.L. Noriega, *Eur. Phys. J.* **C49** (2007), 315
J.L. Klay, *Nucl. Phys.* **A787** (2007), 52

- [11] Sjostrand T, Mrenna S, Skands P *JHEP* 0605:026 (2006)
- [12] Marchesini G, Webber B R, Abbiendi G, Knowles I G, Seymour M H, Stanco L *Comput. Phys. Commun.* **67** 465 (1992); Corcella G, Knowles I G, Marchesini G, Moretti S, Odagiri K, Richardson P, Seymour M H, Webber B *JHEP* **0101** 010 (2001); Corcella G, Knowles I G, Marchesini G, Moretti S, Odagiri K, Richardson P, Seymour M H, Webber B hep-ph/0210213
- [13] I.P. Lokhtin, A.M. Snigirev *Eur. Phys. J.* **C45** (2006), 211
- [14] Zapp K, Ingelman G, Rathsman J, Stachel J, Wiedemann U A, *Eur. Phys. J* **C60** 617 (2009)
- [15] Armesto N, Cunqueiro L, Salgado C A, *Eur. Phys. J* **C63** 679 (2009)
- [16] Armesto N, Corcella G, Cunqueiro L, Salgado C A, *JHEP* 0911:122 (2009)
- [17] S.Z. Belenky, *Shower Processes in Cosmic Rays*, Moscow, Gostechizdat, 1948 (in Russian)
- [18] Dremin I M *JETP Lett.* **31** 185 (1980); Dremin I M, Leonidov A V *Sov. Phys. Usp.* **23** 515 (1980); Dremin I M, Leonidov A V *Sov. Journ. Nucl. Phys.* **35** 247 (1982); Dremin I M, Leonidov A V *Sov. Phys. Usp.* **38** 723 (1995)
- [19] Leonidov A V, Ostrovsky D M *Phys. Atom. Nucl.* **60** 110 (1997); Leonidov A V, Ostrovsky D M, *Phys. Atom. Nucl.* **62** 701 (1999)
- [20] B.G. Zakharov, *JETP Lett.* **86** (2007), 444; *ibid.*, **88** (2008), 781
- [21] A.V. Selikhov, M. Gyulassy, *Phys. Lett.* **B316** (1993), 373
A.V. Selikhov, M. Gyulassy, *Phys. Rev.* **C49** (1994), 1726
- [22] G. Bergmann, *Phys. Rep.* **107** (1984), 1
- [23] S. Chakravarty, A. Schmid, *Phys. Rep.* **140** (1986), 195
- [24] G. Bergmann, *Solid State Commun.* **42** (1982), 815
- [25] M. Bengtsson, T. Sjostrand, *Nucl.Phys.* **B289** (1987), 810
- [26] L.D. Landau, *Journal of Physics USSR* **8** (1944), 204
- [27] P.V. Vavilov, *JETP* **32** (1957), 920
- [28] A.H. Muller, *Phys. Lett.* **B104** (1981) 161